Journal of Fluorescence (2019) 29:195–201
https://doi.org/10.1007/s10895-018-2328-y

ORIGINAL ARTICLE

A Dicyanomethylene-4H-Pyran Based NIR Ratiometric Fluorescent Probe for Diazane and its Bioimaging

Gongchun Li[1] · Yongxiang Liu[2] · Xiaopeng Yang[2] · Yong Ye[2]

Received: 2 October 2018 / Accepted: 22 November 2018 / Published online: 29 November 2018

Abstract
A near-infrared ICT-based fluorescent probe LX was successfully obtained. LX which detection limit is low as 22.2 nm shows excellent selectivity and high sensitivity to diazane. LX can selectively detected diazane from other species over a wide pH (3–10) range. A obvious color change of solution from yellow to orange can be found, allowing the naked eye to detect. The sensing mechanism was reasonably detected by ESI-MS and DFT calculations. In addition, LX succeed in the visualization of diazane in living cells and the detection of diazane in water samples.

Keywords Fluorescent probe · Diazane · NIR · ICT

Introduction

Diazane, also named as hydrazine (N_2H_4) is an important active base and reducing agent, and has a wide range of applications in the chemical industry, medicine and farm chemical [1]. It plays an important role in ruducer, anti-corrosive, pharmaceutical intermediates, textile dyes, and so on [2]. Diazane is often used in missiles and rocket propulsion systems as propellants due to their durability and explosiveness [3]. It is also used for the synthesis of herbicides and plant growth regulators [4]. Although diazane is useful, diazane and its aqueous solutions are harmful to the health of people and animals, and can cause serious environmental problems [5]. What's more, it is easily absorbed by the mouth, skin and inhalation during production, use, transportation and disposal, causing serious harm to the lungs, cerebrospinal axis, kidney and liver. Therefore, it is important to establish reliable methods for diazane detection with good sensitivity and selectivity.

Commonly used detection methods for diazane include flow detection [6, 7], electrochemistry [8], chemiluminescence [9, 10], fluorescence spectroscopy [11, 12], chromatography [13], gas chromatography [14], high-efficiency liquid phase chromatography [15] and capillary electrophoresis [16]. However, most of above means are effective for extracellular diazane detection and require a sample preparing steps. Only a few of these means can be used to detect intracellular diazane. Differ from them, fluorescent probes become a powerful method for monitoring the extracellular and intracellular levels of various biologically related species and understanding their function due to their fast, non-destructive, selective and sensitive emission signal advantages. Various diazane fluorescent probes have been reported so far [17–27]. In these reports, most probes show emission and absorption in the ultraviolet or visible range and are not suitable for bioimaging. Near-infrared (NIR) fluorescent probes are highly desirable because light in the NIR region exhibits lower background fluorescence, deeper penetration, and lower phototoxicity [28, 29]. Few probe for diazane based on NIR dyes were designed. The cyanine probe developed by Peng and colleagues showed good selectivity and a low detection limit [30]. In addition, Zhang's team designed a near-infrared fluorescent sensor for monitoring diazane [31]. The excellent properties of these sensors include obvious "turn on"

Electronic supplementary material The online version of this article (https://doi.org/10.1007/s10895-018-2328-y) contains supplementary material, which is available to authorized users.

✉ Yong Ye
yeyong03@tsinghua.org.cn

[1] Key laboratory of Chemo/Biosensing and Detection, College of Chemistry and Chemical Engineering, Xuchang University, Xuchang 461000, China

[2] College of Chemistry and Molecular Engineering, Zhengzhou University, Zhengzhou, China

response, good selectivity and high sensitivity. However, these sensors also have some other shortcomings, e.g. complex synthesis, low efficiency, and so forth.

On the other hand, ratio chemical sensors can give built-in correction of environmental factors through measuring change in the emission intensity ratio at two different wavelengths [32, 33]. From this perspective, sensors based on fluorescence resonance energy transfer (FRET) and intramolecular charge transfer (ICT) are the most valuable. Generally, the synthetic routes of the FRET-based probes are long. They also require a strong spectral overlap between the acceptor's absorption and the donor's emission. The ICT-based proportional fluorescent probe has the advantages of simple synthesis and large emission shift. However, to date, studies of ICT-based proportional fluorescent sensors for diazane working in NIR are still very limited.

Here, we present a NIR ratio fluorescent sensor LX to detect diazane with the largest Stokes shift (Scheme 1). The LX probe has high sensitivity and selectivity, and the detection limit is 22.8 nm. In addition, fluorescent imaging experiments on diazane in SMMC-7721 cells indicate its practical application in biological systems.

Experimental

Materials

Fluorescent spectroscopy was recorded on a Hitachi F-4600 fluorescence spectrophotometer and the excitation and emission wavelengths were set to 10.0 nm. The UV-visible spectrum was measured with an Agilent 8453 spectrophotometer. ^{1}H and ^{13}C NMR spectra were performed on a Bruker-DTX-400 spectrometer and TMS used as an internal reference. ESI-MS was performed by an HPLC Q-Tof HR-MS spectrometer. All synthetic materials were purchased from commercial suppliers and directly used. The solvent used in this paper was purified according to standard procedures. A stock solution (10 mM) of LX was prepared by dissolving the amount required in DMSO. A stock solution of the other anion (10 mM) was prepared from the corresponding inorganic salt.

Synthesis

Synthesis of 2-(2-Methyl-4H-Chromen-4-Ylidene) Malononitrile

The synthesis of 2-(2-methyl-4H-chromen-4-ylidene) malononitrile is based on the reported method [16].

Synthesis of Probe LX

134.0 mg terephthaldehyde (1.0 mmol) and 208 mg 2-(2-methyl-4H-chromen-4-ylidene) malononitrile (1.0 mmol) was mixed in 15 mL of absolute ethanol. Piperidine (1.0 mmol) was then added. Above mixture was heated to reflux under nitrogen. The reaction was checked by TLC until completed. Then, reaction solution was cooled to room temperature. After solvent was removed by reduced pressure, crude product was obtained. Purified by by column chromatography on silica gel (using CH_2Cl_2:PE = 3:1, and then CH_2Cl_2), compound LX was given as a yellow solid. Yield 52%. mp: 319–320 °C. ^{1}H NMR ($CDCl_3$, 400 MHz, ppm): 10.06 (s, 1 H), 8.94 (d, J = 8.36 Hz, 1H),7.96 (d, J = 7.64 Hz, 2 H),7.75 (d, J = 7.92 Hz, 3 H),7.66 (d, J = 16.04 Hz, 1 H),7.58 (d, J = 8.44 Hz, 1 H),7.49 (t, J = 8.16 Hz, 1 H),6.96 (d, J = 13.96 Hz, 2 H); ^{13}C NMR ($CDCl_3$, 100 MHz, ppm): 191.301, 156.374, 152.575, 152.259, 140.211, 137.143, 136.886, 134.946, 130.395, 128.330, 126.240, 125.914, 121.872, 118.659, 116.411, 115.354, 108.085, 99.982. HR-MS: m/z, calculated for $C_{21}H_{13}N_2O_2^+$ $[M+H]^+$ 325.0972; Found 325.0977.

Results and Discussion

Probe LX was synthesized from dicyanomethylbenzopyran and terephthalaldehyde. Its structure was confirmed by ^{1}H NMR, ^{13}C NMR and HR-MS spectroscopy (Fig. S1–3). Using this probe, we begin study its absorption spectra changes on the addition of diazane and other biologically relevant analytes (eg, Ac-, Cl-, Br-, I-, NO_3-, SO_3^{2-}, SO_4^{2-}, HCO_3-,

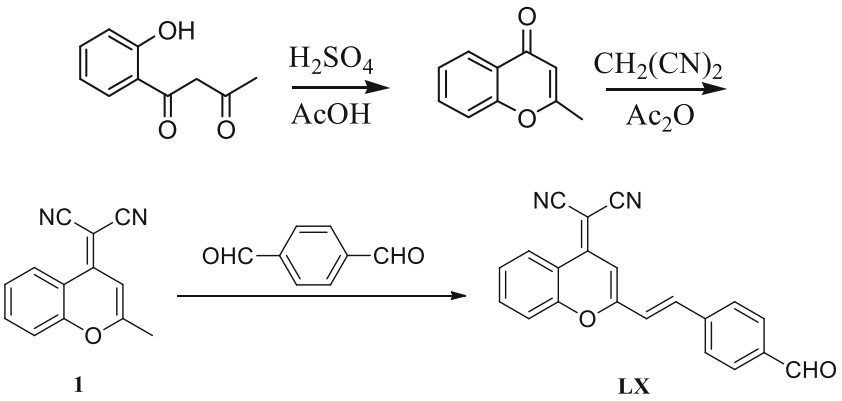

Scheme 1 Synthetic route of title compound **LX**

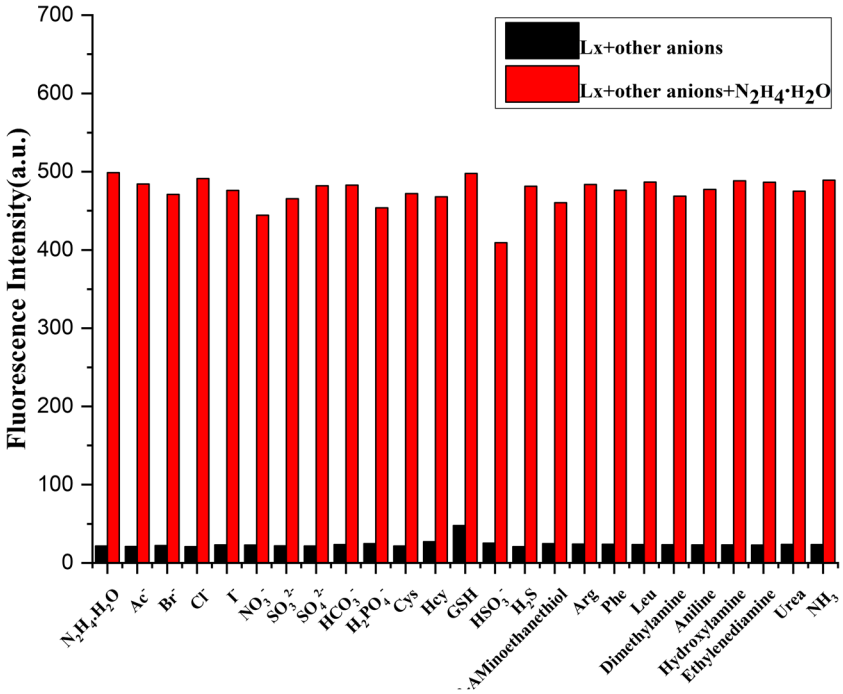

Fig. 1 The interference analyzes of LX in DMSO / PBS buffer (10 mM, pH 7.4) at 25 °C (λex = 460 nm. Slit: 10.0 nm). The black bar represents the fluorescence of LX (10 μM) and the 10 equivalent other analytes. The red bar shows the fluorescence of solution, after 10 equivalent of $N_2H_4.H_2O$ was added to the solution of LX (10 μM) and other analytes (10 equivalent)

HSO_3-, H_2PO_4-, H_2S, Cys, Hcy, GSH, 2-aminoethanol, Arg, Phe, Leu, dimethylamine, aniline, hydroxylamine, ethylenediamine, urea and NH_3) in DMSO/ PBS solution (10 mM, pH 7.4) at 25 °C. Free probe LX exhibited maximum absorption at 420 nm (shown in Fig. S4). After the addition of diazane, the absorption at 420 nm was significantly reduced. A new absorption at 452 nm was found. Along with the 32 nm red shift behavior, the color of the solution changes from yellow to orange (Fig. S5), allowing the colorimetric detection of diazane. Other biologically relevant analytes could not cause this kind of absorption changes. The absorption of LX (10 μM) in the presence of different concentrations of N2H4.H2O were also measured (Fig. S6). The absorption peaks at 420 nm and 448 nm simultaneously disappeared,

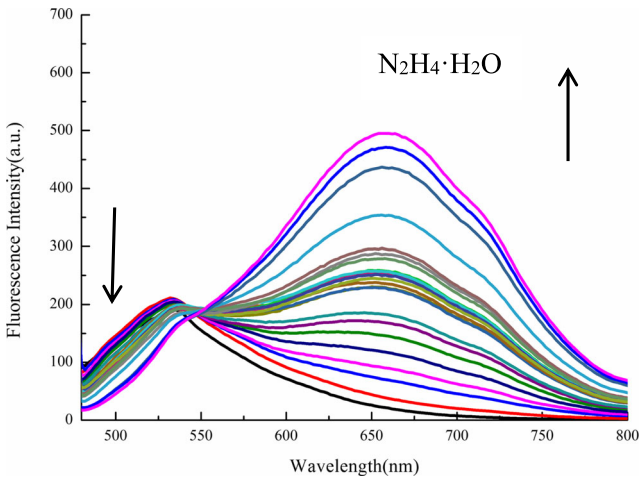

Fig. 2 Fluorescent emission of LX (10 μM) in the presence of 0–10 equiv. of $N_2H_4{\cdot}H_2O$ in DMSO/water solution. (Slits: 10.0 nm, λ_{ex} = 460 nm)

and a new maximum absorption peaks red shift to 452 nm after the addition of 10 equiv. hydrazine.

The selectivity of LX to $N_2H_4.H_2O$ was further observed in the fluorescence spectrum. As shown in Fig. S7, at 460 nm excitation, the alone detector LX shown a weak emission at approximately 532 nm. When 10 eq. of analytes added, such as Br-, I-, AC-, Cl-, NO_3-, SO_3^{2-}, HCO_3-, HSO_3-, H_2PO_4-, H_2S, Cys, Hcy, GSH, 2-aminoethanethiol, Arg, Phe, Leu, dimethylamine, aniline, hydroxylamine, ethylenediamine, urea, and NH_3, no obvious change in fluorescence intensity was shown. Under the same conditions, as $N_2H_4{\cdot}H_2O$ was added, the emission at 532 nm decreased, and a new characteristic fluorescence of the emission band centered at 660 nm enhanced quickly. A large Stokes shift of 200 nm was observed. It has a larger Stokes shift than most of the reported diazane probes. In addition, other competitive analytes (eg, Ac-, Cl-, Br-, I-, NO_3-, SO_3^{2-}, SO_4^{2-}, HCO_3-, HSO_3-, H_2PO_4-, H_2S, Cys, Hcy, GSH, GSH, 2-aminoethanethiol, Arg, Phe, Leu, dimethylamine, aniline, hydroxylamine, ethylenediamine, urea, and NH_3) binding studies shown in Fig. 1 clearly established non-interference effect of other analytes (10 equivalents) on the selective detection of probe LX to $N_2H_4H_2O$.

In general, it is a very important to evaluate the detection limit of new probes. Subsequently, we detected the sensitivity of LX to $N_2H_4{\cdot}H_2O$ by changing the concentration of $N_2H_4{\cdot}H_2O$ (0–100 μM) (Fig. 2). The free probe LX displays an fluorescent emission at 532 nm. As the concentration of $N_2H_4{\cdot}H_2O$ increases, the fluorescence intensity at 660 nm increases. At the same time, there is a fluorescence intensity decrease at 532 nm. In order to understand sensitivity of LX,

Scheme 2 The present mechanism of **LX** to diazane

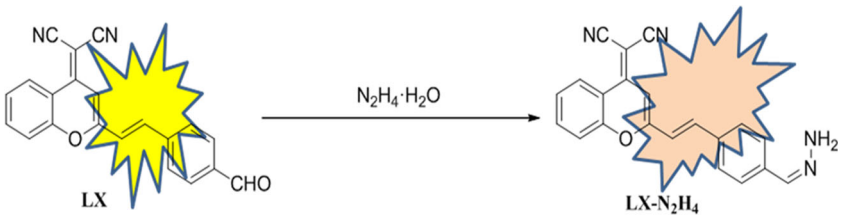

its detection limit for $N_2H_4·H_2O$ was determined by fluorescence titration (Fig. S8). The change in the fluorescence intensity ratio 532 nm/660 nm is linear with the concentration of $N_2H_4·H_2O$ in the range of 0 to 10 μM ($R^2 = 0.99948$). Therefore, under the experimental conditions, the detection limit of LX for $N_2H_4·H_2O$ is 22.2 nM, indicating that LX could be used as a highly sensitive detector for $N_2H_4·H_2O$ quantitative detection.

In order to obtain the best applicable pH range, the fluorescent intensity of LX and LX + $N_2H_4·H_2O$ at different pH values was studied. The weak fluorescent intensity of alone LX (10 μM) did not change significantly from pH 2.0 to pH 13.0, meaning that LX was stable. However, a significant change in fluorescence was given in the presence of 10 equivalents of $N_2H_4·H_2O$. Fluorescence of LX + $N_2H_4·H_2O$ is stable between pH 3 and 10 (Fig. S9). Therefore, a physiological pH 7.4 was applied in following experiment. LX showed a broader pH range than previously reported [19, 21, 23]. These results show that LX can detect $N_2H_4·H_2O$ with good sensitivity between pH 3 and 10.

The fluorescence stability of LX and the reaction time process of LX for $N_2H_4·H_2O$ were measured (Fig. S10). No change in fluorescence was observed within 110 min, which means that LX was stable. After adding 10 equal

Fig. 3 The HOMO/LUMO energy levels and interfacial plots of the orbitals for LX and product LX-N_2H_4

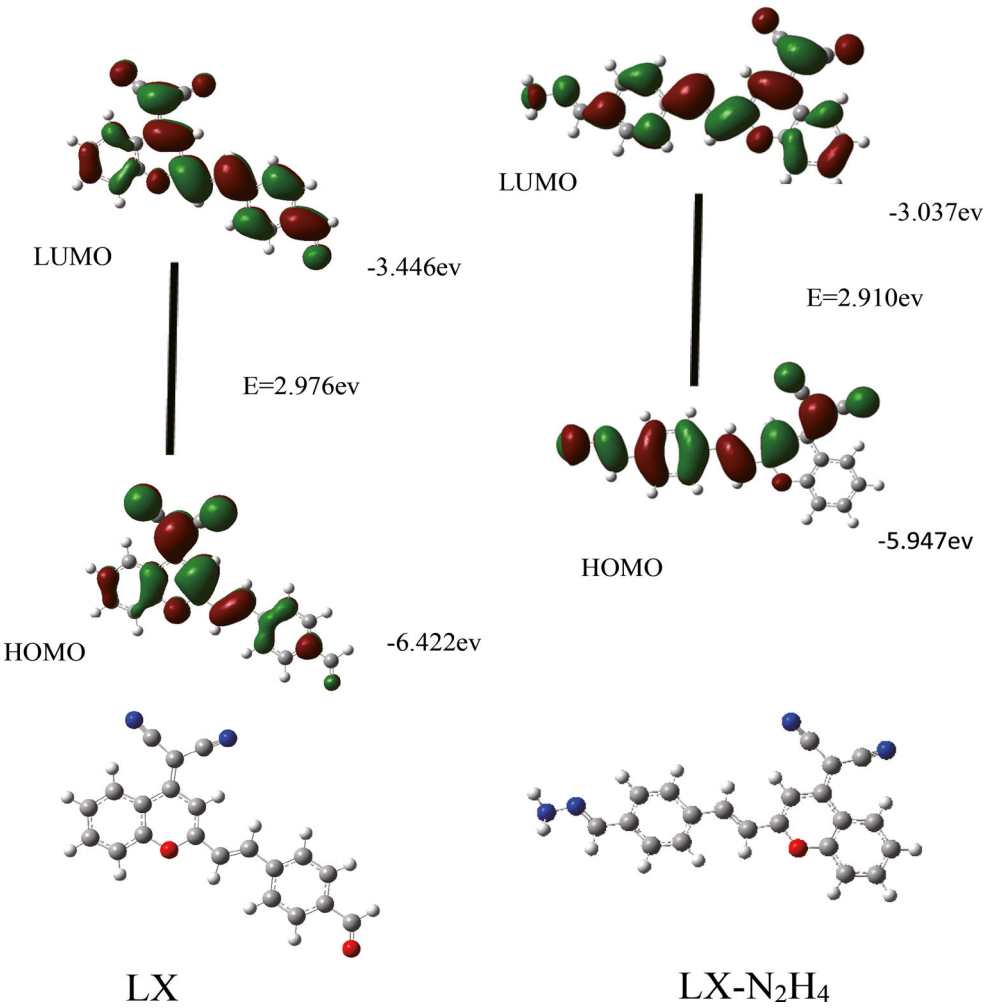

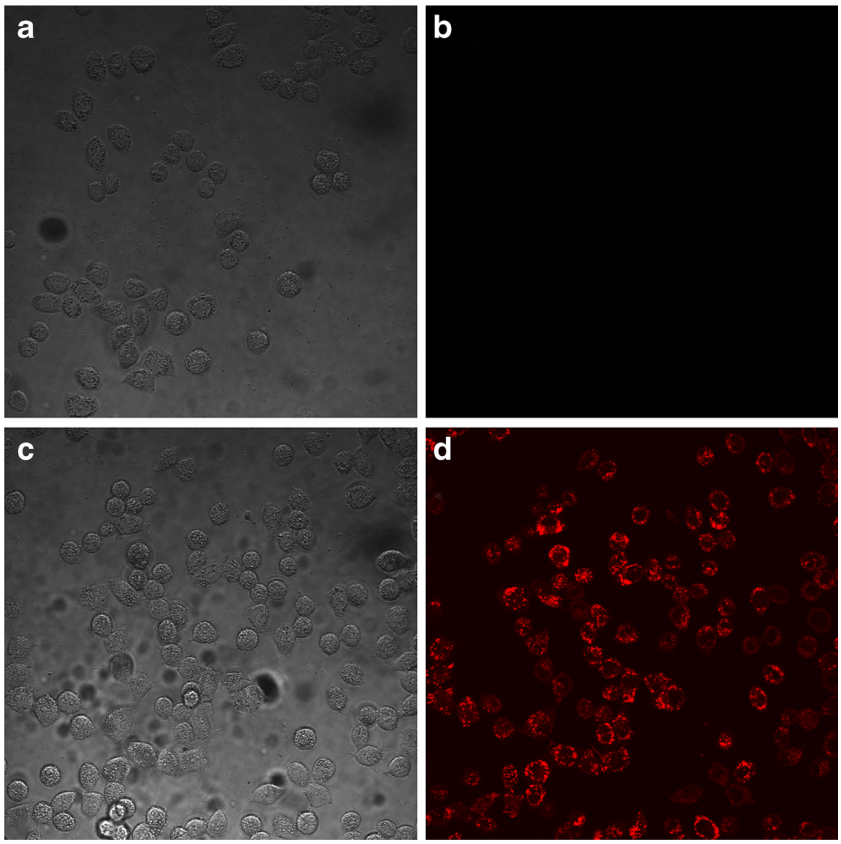

Fig. 4 Confocal fluorescence images of $N_2H_4{\cdot}H_2O$ with probe LX in ECa9707 cells. (**a**, **b**) ECa9707 cells pretreated with LX (5 μM) for 30 min. (**c**, **d**) ECa9707 cells were pretreated with probe LX (5 μM) for 30 min and then incubated with $N_2H_4{\cdot}H_2O$ (10 μM) for 2 h. Cells were imaged using OLYMPUS FV10 confocal microscope

amounts of $N_2H_4{\cdot}H_2O$ to the probe LX solution, the fluorescence emission intensity increased slowly and reached a maximum at 110 min.

To explore the sensing mechanism of LX, the ^{1}H NMR spectrum of LX in $DCCl_3$ was investigated. LX gave a sharp single peak at 10.06 ppm (Fig. S1) due to the aldehyde group. From the ^{1}H NMR spectra of the LX with diazane (Fig. S11), it can be found that the proton signal at 10.06 ppm was disappeared, after the addition of diazane. This means that part of the aldehyde group changed to the hydrazone. The detecting mechanism of LX was also studied by ESI-MS. The detector LX shows a peak at *m/z* 325.0977 (assigned to $C_{21}H_{13}N_2O_2^+$, $[M + H^+]$) (Fig. S3). The ESI-MS analysis of the reaction mixture of LX with diazane revealed that the peak of *m/z* 325.0977 vanished. A new significant peak was found at *m/z* 339.1244 and assigned to $[LX\text{-}H_2O + N_2H_4]^+$ (corresponding to $C_{21}H_{15}N_4O^+$, $[M + H^+]$) (Fig. S12). In view of the above results, it is assumed that the sensing mode of LX is assumed to be Scheme 2. LX is weakly fluorescent due to the suppression of the ICT process. Upon reaction with diazane, the aldehyde group of LX becomes a hydrazone group, and the ICT process occurs due to the powerful electron contribution of the amino group, resulting in an increase in fluorescence.

To further confirm our hypothesis of the detection mechanism, the density function theory (DFT) was used to examine LX and its corresponding product LX-N_2H_4 using the cc-pvTZ basis set. Comparing the level changes in HOMO and LUMO of LX and its corresponding product LX-N_2H_4 respectively, it was found that the levels of HOMO and LUMO all increased due to the ICT effect. HOMOs has increased even more. For the probe LX and the corresponding product, the HOMO–LUMO energy gap was calculated to be 2.976 eV and 2.910 eV, respectively, as shown in Fig. 3. Furthermore, the HOMO-LUMO energy gap of LX-N_2H_4 is smaller than that of LX. This is very consistent with the red shift of the absorption observed, when LX is treated with diazane (Fig. S5).

This paper also discusses the practical application of LX in the detection of $N_2H_4{\cdot}H_2O$, because $N_2H_4{\cdot}H_2O$ is a distrusted carcinogen and is widely applied in various industrial processes. First, we used LX to measure trace amounts of $N_2H_4{\cdot}H_2O$ in distilled water, tap water, river water, and lake water. Equal amounts of $N_2H_4{\cdot}H_2O$ were added to different waters and the pH of solution was tuned to 7.4. Four kind of water samples which concentrations of $N_2H_4{\cdot}H_2O$ are 10, 20, 30, 40, 50, 60, 70 and 80 μM were studied (Fig. S13). The results show that the measurement results are consistent with the actual amount of $N_2H_4{\cdot}H_2O$, which confirms that the LX is effective detector for $N_2H_4{\cdot}H_2O$ in actual water samples.

Then, we investigated the detecting ability of probes LX to $N_2H_4{\cdot}H_2O$ in living cells. Firstly, it is important to examine the cytotoxic effects of LX and $N_2H_4{\cdot}H_2O$ and their

complexes on SMMC-7721 cells. The cytotoxicity of LX and $N_2H_4{\cdot}H_2O$ at different concentrations was examined by the established MTT method. We seeded cells into 96-well plates at a density of 5×10^3 cells/well. Then different concentrations of LX and $N_2H_4{\cdot}H_2O$ were incubated for 24 h. Each group of three established wells, and the blank control group did not have a drug intervention group were set up. The results showed that LX have some cytotoxicity and its cytotoxicity higher than $N_2H_4{\cdot}H_2O$ (Fig. S14). When 5 μM of LX was used, about 80% cells were keep well. Although the toxicity of diazane to mammalian cells has been reported[52], title compound is still a useful detector for researching biological processes involving diazane in living cells.

In order to grope for the potential applications of LX in biological samples, fluorescent imaging of LX in living cells was also investigated. As shown in Fig. 4b, no fluorescence was appeared under the fluorescent microscope when ECa9707 cells were incubated with 5 μM of LX. After ECa9707 cells were pretreated with 10 μM of $N_2H_4{\cdot}H_2O$ for 2 h, then with 5 μM of LX, a strong red fluorescence (Fig. 4d) appeared. This proved that LX could be used for $N_2H_4{\cdot}H_2O$ detection in living cells.

Conclusions

In conclusion, we developed an ICT-based NIR ratio probe LX that selectively detects traces of $N_2H_4{\cdot}H_2O$ in vitro and in water samples. LX exhibited a significant change in the intensity ratio of the emission spectrum caused by $N_2H_4{\cdot}H_2O$. In addition, LX has a wider pH range and a lower detection limit. LX has also been successfully applied to bioimaging of $N_2H_4{\cdot}H_2O$ in living cells. We hope this new ICT-based detector LX could be used in a variety of biological and chemical applications.

Acknowledgements This work was financially supported by NSFC (No. 21572209) and Program for Innovative Research Team (in Science and Technology) in University of Henan Province (No. 17IRTSTHN002).

References

1. Ragnarsson U (2001) Synthetic methodologyfor alkyl substituted hydrazines. Chem Soc Rev 30:205–213
2. Wang J, Chen L (1995) Hydrazine detection using a tyrosinase-based inhibition biosensor. Anal Chem 67:3824–3827
3. Zelnick SD, Mattie DR, Stepaniak PC (2003) Occupational exposure to hydrazines: treatment of acute central nervous system toxicity. Aviat Space Environ Med 74:1285–1291
4. Zhang B, Yang X, Zhang R, Liu Y, Ren X, Xian M, Ye Y, Zhao Y (2017) A lysosomal-targeted two-photon fluorescent probe to sense hypochlorous acid in live cells. Anal Chem 89:10384–10390
5. Brown AB, Gibson TL, Baum JC, Ren T, Smith TM (2005) Fluorescence-enhancement sensingof ammonia andhydrazines via disruption of the internal hydrogen bond in a carbazolopyridinophane. Sensors Actuators B Chem 110:8–12
6. Feng W, Qiao Q, Leng S, Miao L, Xu Z (2016) A 1,8-naphthalimide-derived turn-on *fluorescentprobe* for imaging lysosomal nitric oxide in living cells. Chin Chem Lett 27:1554–1558
7. Li J, Yang X, Zhang D, Liu Y, Tang J, Li Y, Zhao Y, Ye Y (2018) A fluorescein-based "turn-on" fluorescence probe for hypochlorous acid detection and its application in cell imaging. Sensors Actuators B Chem 265:84–90
8. Batchelor-McAuley C, Banks CE, Simm AO, Jones TGJ, Compton RG (2006) The electroanalytical detection of hydrazine: a comparison of the use of palladium nanoparticles supported on boron-doped diamond and palladium platedBDD microdisc array. Analyst 131:106–110
9. Collins GE, Latturner S, Rose-Pehrsson SL (1995) Chemiluminescence detection of hydrazine vapor. Talanta 42:543–551
10. Safavi A, Baezzat MR (1998) Flow injection chemiluminescence determination ofhydrazine. Anal Chim Acta 358:121–125
11. Collins GE, Rose- Pehrsson SL (1993) Sensitive, fluorescent detection of hydrazine via derivatization with 2,3-naphthalene dicarboxaldehyde. Anal Chim Acta 284:207–215
12. Collins GE, Rose-Pehrsson SL (1994) Fluorescent detection of hydrazine, monomethylhydrazine, and1,1-dimethylhydrazine by derivatization with aromatic dicarbaldehydes. Analyst 119:1907–1913
13. Elder DP, Snodin D, Teasdale A (2011) Control and analysis of hydrazine, hydrazides and hydrazones- genotoxic impurities in active pharmaceutical ingredients (APIs) and drug products. J Pharm Biomed Anal 54:900–910
14. Sun M, Bai L, Lui DQ (2009) A generic approach for the determination of trace hydrazine in drug substances using in situ derivatization-headspace GC–MS. J Pharm Biomed Anal 49:529–533
15. Li S, Zhang D, Xie X, Ma S, Liu Y, Xu Z, Gao Y, Ye Y (2016) A novel solvent-dependently bifunctional NIR absorptive and fluorescent ratiometric probefor detecting Fe^{3+}/Cu^{2+} and its application in bioimaging. Sensors Actuators B Chem 224:661–667
16. Liu J, Zhou W, You T, Li F, Wang E, Dong S (1996) Detection of hydrazine, methylhydrazine, and isoniazid by capillary electrophoresis with a palladium- modified microdisk array electrode. Anal Chem 68:3350–3353
17. Goswami S, Aich K, Das S, Roy SB, Pakhira B, Sarkar S (2014) A reaction based colorimetric as well as fluorescence 'turn on' probe for the rapid detection of hydrazine. RSC Adv 4:14210–14214
18. Qian Y, Lin J, Han L, Lin L, Zhu H (2014) A resorufin-based colorimetric and fluorescent probefor live-cell monitoring ofhydrazine. Biosens Bioelectron 58:282–286
19. Yang X, Liu Y, Wu Y, Ren X, Zhang D, Ye Y (2017) A NIR ratiometric probe for hydrazine "naked eye" detection and its imaging in living cell. Sensors Actuators B Chem 253:488–494
20. Xiao L, Tu J, Sun S, Pei Z, Pei Y, Pang Y, Xu Y (2014) A fluorescent probe for hydrazine and its in vivo applications. RSC Adv 4: 41807–41811
21. Zhang L, Zhu H, Zhao C, Gu X (2017) A near-infrared *fluorescent* probe for monitoring fluvastatin-stimulated endogenous H_2S production. Chin Chem Lett 28:218–221
22. Zhao Z, Zhang G, Gao Y, Yang X, Li Y (2011) A novel detection technique of hydrazine hydrate: modality change of hydrogen bonding-induced rapidand ultrasensitive colorimetric assay. Chem Commun 47:12816–12818
23. Choi M, Moon J, Bae J, Lee J, Chang S (2013) Dual signaling of hydrazine by selective deprotection of dichlorofluorescein and resorufin acetates. Org Biomol Chem 11:2961–2965
24. Jin X, Liu C, Wang X, Huang H, Zhang X, Zhu H (2015) A flavone-based ESIPT fluorescent sensorfor detection of N_2H_4 in aqueous solution and gas state and its imaging in living cells. Sensors Actuators B Chem 216:141–149

25. Yu S, Wang S, Yu H, Feng Y, Zhang S, Zhu M, Yin H, Meng X (2015) A ratiometric two-photon fluorescent probefor hydrazine and its applications. Sensors Actuators B 220:1338–1345
26. Lee MH, Yoon B, Kim JS, Sessler JL (2013) Naphthalimide trifluoroacetyl acetonate:a hydrazine selective chemodosimetric sensor. Chem Sci 4:4121–4126
27. Chen W, Liu W, Liu XJ, Kuang YQ, Yu RQ, Jiang JH (2017) A novel fluorescent probe for sensitive detection and imaging of hydrazine in living cells. Talanta 162:225–231
28. Yuan L, Lin W, Zhao S, Gao W, Chen B, He L, Zhu S (2012) A unique approach to development of near- infrared fluorescent sensorsfor in vivo imaging. J Am Chem Soc 134:13510–13523
29. Guo Z, Park S, Yoon J, Shin I (2014) Recent progress in the development of near-infrared fluorescent probesfor bioimaging applications. Chem Soc Rev 43:16–29
30. Hu C, Sun W, Cao J, Gao P, Wang J, Fan J, Song F, Sun S, Peng X (2013) A ratiometric near-infrared fluorescent probe for hydrazine and its in vivo applications. Org Lett 15:4022–4025
31. Zhang J, Ning L, Liu J, Wang J, Yu B, Liu X, Yao X, Zhang Z, Zhang H (2015) Naked-eye and near- infrared fluorescence probe for hydrazine and its applications in in vitro and in vivo bioimaging. Anal Chem 87:9101–9107
32. Fan J, Sun W, Hu M, Cao J, Cheng G, Dong H, Song K, Liu Y, Sun S, Peng X (2012) An ICT-based ratiometric probe for hydrazine and its application in live cells. Chem Commun 48:8117–8119
33. Wang C, Liu Y, Cheng J, Song J, Zhao Y, Ye Y (2015) Efficient FRET-based fluorescent ratiometric chemosensors for Fe^{3+} and its application in living cells. J Lumin 157:143–148